

Watching One's P's and Q's: Promiscuity, Plasticity, and Quasiequivalence in a $T = 1$ Virus

Michael S. Chapman

Department of Chemistry and Institute of Molecular Biophysics, Florida State University, Tallahassee, Florida 32306-4380 USA

ABSTRACT Although quasiequivalence is not needed to explain the assembly of the $T = 1$ canine parvovirus capsid, the interactions of the 60-fold symmetrical capsid protein with less symmetrical viral components illustrate the elements of plasticity and promiscuity of interactions that are embodied in quasiequivalence. The current analysis is based on interactions of fivefold related proteins with a single peptide running along the fivefold axis, and on interactions of the capsid protein with various fragments of the genomic DNA, each having a different sequence and exposing the protein to interactions with different types of nucleotide base.

INTRODUCTION

Caspar and Klug (1962) introduced the concept of quasiequivalence to explain how polyhedral viruses of different sizes could be assembled from varying numbers of subunits using a minimal number of types of intersubunit contacts. Shells composed of subunits in exactly equivalent environments contain at most 60 subunits, arranged with icosadeltahedral symmetry. An icosadeltahedron can be constructed from an icosahedron by adding vertices at the threefold axes in the centers of each of the 20 triangular faces between fivefold vertices of an icosahedron. In mathematical, architectural, and biological contexts, respectively, Goldberg (1937), Fuller (Marks, 1960), and Caspar and Klug (1962) realized that by alternating fivefold and sixfold vertices of (now) local symmetry in one of several ways, it was possible to construct larger polyhedral shells in which each of the faces (or protein subunits) was in a nearly identical or quasiequivalent environment.

With quasiequivalence, strict symmetrical equivalence is not required (Caspar, 1980), but it was expected that the same chemical interactions between subunits would be used, thereby ensuring specificity of assembly. The requirements of equivalent interactions but nonequivalent positional relationships could be satisfied either by subunits with more than one conformation and/or flexible chemical interactions between subunits (Caspar, 1980). The essentials of nonexact symmetry, specificity of interactions, and protein flexibility predicted many aspects of viral assembly remarkably well. They have been largely validated by atomic resolution structure determinations (see Harrison et al., 1996, for a recent review), although sometimes in ways a little different from what was expected—such as the use of flexible arms to bind together near-identical subunits in

several discretely different configurations (Liddington et al., 1991; Rayment et al., 1982). Similar principles apply throughout much of structural biology and, for example, have recently been invoked as an explanation for the evolution of oligomeric proteins (Bennett et al., 1995).

One reason that large spherical viruses have given insight into general applications is that within a single crystal structure, chemically identical subunits are seen in a variety of conformations or participating in several variants of a chemical interaction. This offers a rare glimpse into the heterogeneity of macromolecular structure and interactions. The $T = 1$ viruses analyzed here are among the simplest, and their 60 subunits can be arranged in a spherical capsid with exact icosahedral symmetry without need of quasiequivalence. Recently, some of the interactions of these highly symmetrical capsids with an asymmetrical environment have been visualized, similarly yielding insights of general relevance into the adaptability of proteins, and further emphasizing that some of the principles of quasiequivalence are not limited to quasiequivalent viruses.

The focus here will be on the incorporation of asymmetrical elements within an otherwise icosahedrally symmetrical capsid, and interactions of a nearly symmetrical capsid with its asymmetrical genome. Analysis of canine parvovirus (CPV) is the most detailed, but data from other viruses suggest that the results are not unique to CPV. In CPV, a small proportion of the capsid proteins have long N-terminal extensions, and it has been possible to model some of the extensions running along the fivefold axes, causing deviations from exact icosahedral symmetry (see below). In both $T = 7$ polyomavirus (Griffith et al., 1992; Liddington et al., 1991) and $T = 1$ bacteriophage $\phi\chi 174$ (McKenna et al., 1994), for each pentameric unit ($5 \times$ VP1 in polyoma and $5 \times$ (F and G proteins) in $\phi\chi 174$), there are single copies of the additional VP2/3 or H proteins (respectively). Partial disordered electron density is seen near the fivefold axes of both viruses, but in these cases it was not possible to build atomic models.

As for viral genomes, little was seen in the first spherical virus atomic structures, perhaps because they can have a

Received for publication 21 March 1997 and in final form 26 August 1997.

In celebration of Don Caspar's 70th Birthday.

Address reprint requests to Dr. Michael S. Chapman, Institute of Molecular Biophysics, Florida State University, Tallahassee, FL 32306-4380. Tel.: 850-644-8354; Fax: 850-644-3257; E-mail: chapman@sb.fsu.edu.

© 1998 by the Biophysical Society

0006-3495/98/01/639/06 \$2.00

different conformation or orientation in different viruses in the crystal, but also because they do not conform to the icosahedral symmetry that is used during phase determination (Rossmann, 1995). Fragments of genomic nucleic acid have now been seen in several virus structures (Chen et al., 1989; Fisher and Johnson, 1993; Larson et al., 1993; McKenna et al., 1994; Tsao et al., 1991), where the nucleic acid is bound to the capsid, and locally forced to approximate icosahedral symmetry. Even in single-stranded (ss) viruses, the fragments are often seen as duplex, and interactions with the protein are primarily through the phosphoribose backbone, which may conform to the icosahedral symmetry. For this analysis, CPV is more interesting, because it is the bases of the ss-DNA that interact with the protein. The sequence does not have 60-fold symmetry; therefore it is interactions with a variety of sequences that are visualized. This then raises questions of whether the protein or nucleic acid structures adapt, or whether the chemical interactions are flexible enough to accommodate different sequences.

Parvoviruses are small $T = 1$ spherical viruses containing ~5000 nucleotides (nt) of ss-DNA genome (Berns, 1996). The autonomous parvoviruses, which include CPV, cause several diseases (Pattison, 1990). The human virus B19 causes childhood fifth disease and can cause panleukopenia and potentially fatal infection of fetuses (Anderson and Török, 1989; Kurtzman et al., 1989). CPV can cause fatal myocarditis and gastroneuritis in puppies (Studdert, 1990).

The first parvovirus structure to be determined was the full CPV capsid at 3.25 Å (Tsao et al., 1991). Each of the 60 subunits shared the canonical "jelly-roll" antiparallel β -barrel topology of small RNA viruses (Rossmann and Johnson, 1989). The major difference was in the insertion of large loops between the β -strands, leading to large protrusions near the threefold axes. The structure of an empty CPV capsid has also been refined to 3.0 Å (Wu and Rossmann, 1993). Capsid structures of related parvoviruses have also been determined: FPV (feline panleukopenia virus) and minute virus of mice (MVM) at ~3 Å resolution (Agbandje et al., 1993; Llamas-Saiz et al., manuscript submitted for publication), and B19 (Agbandje et al., 1994) at 8 Å resolution.

The CPV capsid contains a mixture of three proteins, VP1–3. Their origins and locations are introduced in Figure 1. Much of the discussion of this paper will center on the interactions of the glycine-rich segment with the surrounding fivefold symmetrical β -barrel domains. This region ($G_{22}SGNGSGGG_{30}GGGGSGG_{37}VG_{39}$) starts at the point from which the N-terminus is cleaved during posttranslational modification of VP2 to 3. It also bridges from the 153-residue N-terminal domain (unique to the minority VP1 component) to the β -barrel domain that is common to VP1, 2, and 3. A second focus will be the effects on the protein of the binding of fragments of the ss-DNA. The DNA conformation is unusual—an 11-nt inverted loop in which the phosphates point in toward chelating metal ions, and the bases point out toward the protein (Chapman and Rossmann, 1995). The binding site is on the inside surface of the

capsid, with a footprint that covers nearly one-third of the inner surface and includes regions from several parts of the polypeptide chain. The site is in a valley running between the fivefold and threefold axes between two adjacent fivefold related capsid proteins (Chapman and Rossmann, 1995).

METHODS

The analysis is based on entries 4dpv and 2cas of the Brookhaven Data Bank, which are, respectively, the refined structures of full and empty capsids. The empty capsid structure (2cas) (Wu et al., 1993) had been refined against alternating subsets of the diffraction data, using the reciprocal space methods ProLSQ (Hendrickson, 1985) and Xplor (Brünger et al., 1987). The DNA-containing capsids (4dpv) had been refined by real-space methods (Chapman, 1995; Chapman and Rossmann, 1996) to a free R -factor (Brünger, 1992) of 28% to 2.9-Å resolution. The empty capsids had been refined before free R -factors, but cross-validation of the empty structure versus the diffraction data of DNA-containing particles and vice versa gave free R -factors of ~25% for the protein components of both full and empty particles (Chapman, 1996). The rms coordinate errors are likely similar, and for the full particle are estimated to be 0.5 Å by Luzzati (1952) analysis, using free R -factors (Brünger, 1997).

Special care was taken with refinement of the glycine-rich region running along the fivefold axis of the DNA-containing particles (Xie and Chapman, 1996), to ensure that it was stereochemically reasonable for the peptide to occupy the narrow pore. Usually, only the most egregious close contacts are restrained (if atoms overlap by 0.2–0.4 Å, ignoring the presence of hydrogens). For the glycine-rich region of CPV, targets were used that restrained atoms to be at least ~1 Å farther apart than in typical refinements. The targets were based on van der Waals radii, extended to implicitly account for the average effect of unseen hydrogens (Connolly, 1983; Xie and Chapman, 1996), and weights on close contacts were doubled. It was possible to model all of the residues of the glycine-rich region, although Gly²² and Ser²³ had particularly diffuse electron density. Despite its small contribution to the overall scattering, there was a small but distinct minimum to the free R -factor for the optimal occupancy (dropping by 0.03%) and a corresponding maximum in the correlation coefficient between model and experimental electron density (Xie and Chapman, 1996).

The electron density of the nucleic acid was the average of up to 60 fragments. As there are no sequences repeated 60 times within the genome, the density represented the superimposition of fragments of different sequences. Apparently there is some low-level specificity, because the bases of some positions distinctly resembled particular base types (Chapman and Rossmann, 1995) and were not featureless, as would be expected of randomly selected frag-

ments. For each nucleotide, the prevalent base type was guessed from the shape of the electron density and possible steric overlap. The guessed sequence (XTACCTCTTGC; Chapman and Rossmann, 1995) of the refined nucleotide might resemble a consensus sequence, but need not be the actual chemical sequence of any part of the CPV genome.

With both the glycine-rich region and the oligonucleotide, a single atomic model is being used to represent a set of structures. At most one in five of the capsid proteins has a glycine-rich segment passing through the fivefold pore. The electron density represents the average of the five possible configurations, of which one was arbitrarily selected for refinement, so that the pore would not be forced to be more open than needed (through stereochemical restraints). The electron density averaged about the five possible orientations is blurred, and the model for the glycine-rich region is therefore plausible, but is likely to be less precise than in other regions of the structure. The nucleic acid model also represents the supposition of fragments of different sequence, but shows fewer characteristics of disorder, because the model represents the prevalent structure and not one of five equals.

RESULTS AND DISCUSSION

Unlike the empty capsids, some of the N-terminal glycine-rich peptides emerge from the fivefold pores in DNA-containing capsids. Evidence for the internal location of empty capsid N-termini is both crystallographic and biochemical. No electron density is seen on the fivefold axes of empty capsids (Wu and Rossmann, 1993), and only DNA-containing (related) parvoviruses are susceptible to *in vitro* proteolysis that mimics the natural VP1/2 to VP3 cleavage (Clinton and Hayashi, 1976; Tattersall et al., 1977). Although adjustments to the fivefold pore would be required to accommodate the glycine-rich polypeptide within the empty capsid structure, the adjustments are modest (Table 1). The observed root mean square (rms) difference between full and empty capsid fivefold pore-lining residues sur-

rounding the glycine-rich peptide is 0.65 Å. This is calculated from a single structure representing both occupied and vacant pores in the crystal. Dividing this difference by the experimentally determined occupancy (0.65; see caption to Fig. 1) gives an estimate of the change for occupied pores of 1.0 Å, slightly more than the overall difference between the structures (0.62 Å), and the estimate of precision (0.5 Å). Thus the additional polypeptide is accommodated with modest changes to the pore.

The shape of the glycine-rich segment is likely anisotropic. In an extended conformation, its cross section could be thought of as approximately elliptical, with radii of ~ 2.75 and 2.05 Å, calculated by summing bond and van der Waals lengths along a line through the peptide HNCO atoms and for the CH₂ group, respectively. In some directions, the adjustment of pore-lining residues would need to be ~ 0.7 Å greater than others. In the experimental electron density of the full capsid, we expect to see evidence of several structures, moved by different amounts if the pore is occupied, and not moved if unoccupied. Thus elevation of refined B-factor is expected. The pore-lining residues of the empty capsid are slightly higher than average, and are elevated slightly more in the full capsid, which is qualitatively consistent with this rationale. It would be tempting to suggest that the elevated temperature factors for the empty capsids suggest built-in flexibility to accommodate the glycine-rich segment, but all of these differences in B-factors are less than half a standard deviation, and may not be experimentally significant.

The DNA binding site tells a similar story. B-factors show that the inside surface has only slightly higher than average disorder (Table 1). There is no significant difference in the B-factors of regions in contact with ordered DNA and those that are presumably in contact with unseen, disordered DNA. The changes in the structure due to the presence of DNA are larger than average differences throughout the structure, but only by about half a standard deviation. The small size of structural differences is similar to those observed between empty particles of the bacterio-

TABLE 1 Motion of the pore-lining and DNA-binding site amino acids

Regions common to empty and DNA-containing structures	Full		Empty		Coordinate difference (Å)
	B (Å ²)	rms amplitude motion (Å)	B (Å ²)	rms amplitude motion (Å)	
Mean, all atoms	19.5	0.50	13.4	0.41	0.62
Standard deviation, all atoms	14.2		12.0		0.60
Mean, pore-lining residues (38, 164, 166-7, 169)	24.6	0.56	15.7	0.45	0.63
Mean, atoms: A38Cβ, A38Cγ _{1/2} , L169Cδ ₁ , N166Nδ ₂	33.7	0.65	10.9	0.37	0.42
Mean, Inside surface residues	18.2	0.48	16.7	0.46	0.80
Mean, Residues contacting observed DNA fragments	19.4	0.50	18.6	0.49	0.90

Thermal factors and their equivalent root mean square isotropic motions are shown for atoms that are common to the full and empty structures. Residues 156, 158, and 159, on the outside of the capsid, are likely to be pore-lining, but are not seen in the full capsid structure, and are not included in these statistics. Atoms A38Cβ, A38Cγ_{1/2}, L169Cδ₁, and N166Nδ₂ are those in closest contact with the glycine-rich segment of the atomic model.

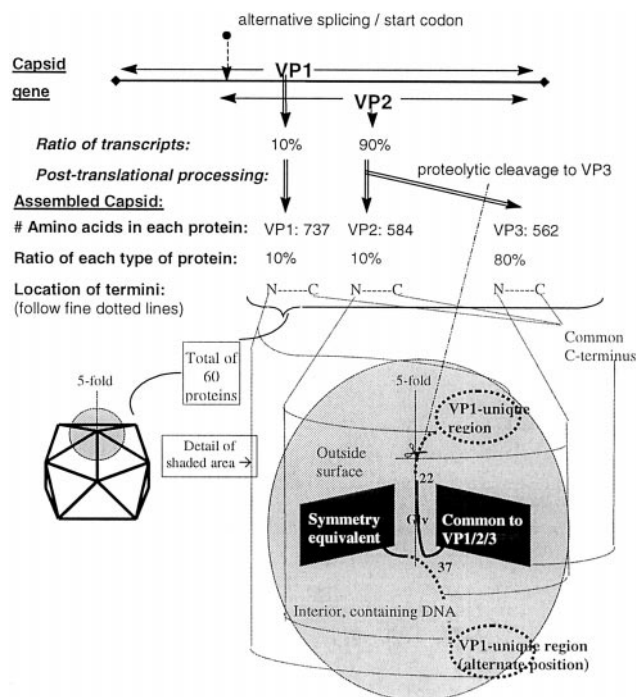


FIGURE 1 Components of the viral capsid. The three capsid proteins, VP1, 2, and 3, are found in an approximately 1:1:10 ratio in mature capsids, but are all derived from the same gene, and they share a common C-terminus. VP1 differs from VP2 in the presence of an additional 153 amino acids resulting from alternative mRNA splicing. The VP1-unique region is not seen in the crystals of CPV. Although by convention, the capsid protein is normally numbered from the VP2 N-terminus, most of VP2 undergoes posttranslational cleavage of the N-terminal 22 residues. The polypeptide to the N-terminal side of the cleavage site is shown by a dashed line because it is not seen in the CPV structure (Xie and Chapman, 1996). Those N-termini that are external are connected to the start of one of the fivefold related β -barrels on the inside capsid surface by a glycine-rich region ($G_{22}SGNGSGGG_{30}GGGGSGG_{37}VG_{39}$) running along the fivefold axis (Tsao et al., 1991). There is room for, at most, one of the five glycine-rich polypeptides in the fivefold axis pore. In fact, the refined occupancy indicates that $13 \pm 2\%$ of the N-termini occupy the pore, or that 65% of the fivefold pores are occupied (Xie and Chapman, 1996). The remaining N-termini are internal and are too disordered to be seen. The crystal structure gives little indication of whether the glycine-rich regions seen in the pores belong to VP1, 2, or 3. However, proteolysis studies indicate that some of the VP1 and two N-termini are external, at least sometimes in DNA-containing particles (but not empty particles) of MVM (Clinton and Hayashi, 1976; Tattersall et al., 1977). Furthermore, the location of epitopes suggests that some VP1 is external in B19 and CPV (Kajigaya et al., 1991; Rimmelzwaan et al., 1990; Rosenfeld et al., 1992), but there is contrary evidence for MVM (Cotmore et al., 1995).

phage MS2 and those containing a 19-nt RNA fragment known to bind at a specific site on the inside surface of the capsid (Valegard et al., 1994).

CONCLUSION

It is of biological importance that many of the features of quasiequivalence are found in a $T = 1$ virus for which quasiequivalence need not be invoked to understand assembly. There are technical reasons why these features were

recognizable in CPV, but may go unrecognized in other macromolecular structure determinations.

Technical

Direct observation of some of CPV DNA, and of the fact that its fivefold pores are filled, shows that the capsid protein is interacting with DNA/peptides that do not share its 60-fold symmetry. Had direct observation not been possible, it would not have been easy to infer the presence of these interactions from their small effects on the capsid protein. The changes in coordinates and B-factors are less than one standard deviation. Because of the power of 60-fold noncrystallographic symmetry (Arnold and Rossmann, 1986) in phase determination, CPV is a very favorable case for which it is possible to visualize protein with only 0.13 occupancy. In fact, map-to-model correlation coefficients (Brändén and Jones, 1990; Jones et al., 1991; Zhou et al., 1997) compare favorably with the recent exceptionally high-quality experimental maps of mannose-binding protein (MBP) A (Burling et al., 1996). This suggests that in more typical protein structures, without the benefit of such high-quality experimental phases, similar low-occupancy alternative conformations might be indiscernible.

Biological

Are the interactions examples of quasiequivalence, promiscuity, or plasticity? Our observations are of the average of at least five structures (fivefold pore) or as many as 60 (DNA binding site). It is not known whether there are rules determining which of the fivefold related capsid proteins have external N-termini. It is not known whether capsid proteins surrounding the pore are designed to adopt one of five distinctly different interactions with a glycine-rich segment, or whether it is designed to be passively accommodating. Thus, at this stage, the CPV interactions lack one fundamental element of quasiequivalence—specificity (Caspar, 1980).

Other elements of the CPV interactions are consistent with theories of quasiequivalence.

Plasticity: Either the structure or interatomic interactions are sufficiently plastic to accommodate a polypeptide with one of five possible orientations.

Plasticity and promiscuity: The protein of the DNA binding site has higher B-factors than average in the empty capsid, but not in the full capsid. (Absolute values are arbitrary, because of scaling.) Thus structural variation (or dynamic motion) of the capsid inner surface appears slightly smaller in the presence of DNA. This, in turn, suggests that the protein is designed to be promiscuous in its chemical interactions without large changes in structure.

Promiscuity

The promiscuity seems to be by design (selection), not accident. It is sufficient to make the binding of CPV

genomic DNA more likely than host nucleic acids (Chapman and Rossmann, 1995). However, the specificity is low enough and promiscuity high enough to allow many different CPV sequences to bind to the 60 symmetry-related binding sites. In this regard it differs from the bacteriophage MS2. The RNA density in the wild-type bacteriophage (Golmohammadi et al., 1993) is much weaker than either that of the MS2 oligonucleotide complex (Valegard et al., 1994) or that of the wild-type CPV (Chapman and Rossmann, 1994). This suggests that MS2 RNA sequences other than the initiation region either do not occupy all of the other symmetry equivalent binding sites of the assembled capsid, or at least bind in somewhat different conformations. This is in contrast to CPV, in which strong DNA density is seen despite the different sequences that must occupy the majority of the symmetry-equivalent capsid binding sites, indicating a high tolerance of different protein-DNA interactions. In MS2, the binding of the specific 19-nt initiation region to capsid protein dimers causes capsid assembly and repression of replicase translation (Beckett and Uhlenbeck, 1988; Witherell et al., 1991). There is, as yet, no evidence of similar specific functions of the DNA binding site in parvoviruses, perhaps accounting for the greater promiscuity seen with CPV.

Because of the high-quality electron density maps available for viruses, it is sometimes possible to detect low occupancy structural features that would be difficult to detect in other systems. With CPV, we see some of the fundamental elements of quasiequivalence—plastic and promiscuous interactions in a system that does not exhibit quasiequivalence itself. This adds to the circumstantial evidence that these principles are pervasive throughout structural biology.

The data on which this analysis is based were obtained in collaboration with Jun Tsao, Mavis Agbandje, Hao Wu, Walter Keller, and Michael Rossmann, while supported by grants to Purdue University from the National Institutes of Health (M. G. Rossmann; AI 11219) and the National Science Foundation (M. G. Rossmann; MCB 9102855).

The current work is supported by grants to Florida State University from the National Science Foundation (MSC; BIR9418741), the American Cancer Society, Florida Division (MSC; F95FSU-2), and the Lucille P. Markey Charitable Trust.

This paper is dedicated to Don Caspar, in celebration of his 70th birthday, to whom the author is indebted. His contribution to the understanding of viral assembly is well known. The *ab initio* phasing essential to the structural determination of CPV built upon earlier successes in the laboratories of Michael Rossmann and Don Caspar, and without such inspiration we might still be trying to solve the structure by more conventional means. The author is very grateful for Dr. Caspar's continuing support and encouragement.

REFERENCES

- Agbandje, M., S. Kajigaya, R. McKenna, N. S. Young, and M. G. Rossmann. 1994. The structure of human parvovirus B19 at 8 Å resolution. *Virology*. 203:106–115.
- Agbandje, M., R. McKenna, M. G. Rossmann, M. L. Strassheim, and C. R. Parrish. 1993. Structure determination of feline panleukopenia virus empty capsids. *Proteins*. 16:155–171.
- Anderson, M. J., and T. J. Török. 1989. Human parvovirus B19. *N. Engl. J. Med.* 321:536–537.
- Arnold, E., and M. G. Rossmann. 1986. Effect of errors, redundancy, and solvent content in the molecular replacement procedure for the structure determination of biological macromolecules. *Proc. Natl. Acad. Sci. USA*. 83:5489–5493.
- Beckett, D., and O. C. Uhlenbeck. 1988. Ribonucleic complexes of R17 coat protein and a translational operator analog. *J. Mol. Biol.* 204:927–938.
- Bennett, M. J., M. P. Schlunegger, and D. Eisenberg. 1995. 3D domain swapping: a mechanism for oligomer assembly. *Protein Sci.* 4:2455–2468.
- Berns, K. I. 1996. *Parvoviridae: the viruses and their replication*. In *Virology*, 3rd Ed. B. N. Fields, D. M. Knipe, P. M. Howley, editors. Raven, New York. 1017–1041.
- Brändén, C.-I., and T. A. Jones. 1990. Between objectivity and subjectivity. *Nature*. 343:687–689.
- Brünger, A. T. 1992. Free *R* value: a novel statistical quantity for assessing the accuracy of crystal structures. *Nature*. 355:472–475.
- Brünger, A. T. 1997. Free *R* value: cross-validation in crystallography. *Methods Enzymol.* 277:366–396.
- Brünger, A. T., J. Kuriyan, and M. Karplus. 1987. Crystallographic *R* factor refinement by molecular dynamics. *Science*. 235:458–460.
- Burling, F. T., W. I. Weis, K. M. Flaherty, and A. Brünger. 1996. Direct observation of protein solvation and discrete disorder using experimental crystallographic phases. *Science*. 271:72–77.
- Caspar, D. L. D. 1980. Movement and self-control in protein assemblies. *Biophys. J.* 32:103–138.
- Caspar, D. L. D., and A. Klug. 1962. Physical principles in the construction of regular viruses. *Cold Spring Harb. Symp. Quant. Biol.* 27:1–24.
- Chapman, M. S. 1995. Restrained real-space macromolecular atomic refinement using a new resolution-dependent electron density function. *Acta Crystallogr.* A51:69–80.
- Chapman, M. S. 1996. Cross-validation *R*-factors and their use in comparing the qualities of refined models for the DNA-containing and empty capsids of canine parvovirus. *Acta Crystallogr.* D52:140–142.
- Chapman, M. S., and M. G. Rossmann. 1995. Single-stranded DNA-protein interactions in canine parvovirus. *Structure*. 3:151–162.
- Chapman, M. S., and M. G. Rossmann. 1996. Structural refinement of the DNA-containing capsid of canine parvovirus using *RSRef*, a resolution-dependent stereochemically restrained real-space refinement method. *Acta Crystallogr.* D52:129–142.
- Chen, Z., C. Stauffacher, Y. Li, T. Schmidt, W. Bomu, G. Kamer, M. Shanks, G. Lomonosoff, and J. E. Johnson. 1989. Protein-RNA interactions in an icosahedral virus at 3.0 Å resolution. *Science*. 245:154–159.
- Clinton, G. M., and M. Hayashi. 1976. The parvovirus MVM: a comparison of heavy and light particle infectivity and their density conversion in vitro. *Virology*. 74:57–63.
- Connolly, M. L. 1983. Solvent accessible surfaces of proteins and nucleic acids. *Science*. 221:709–713.
- Cotmore, S., A. D'Abramo, J. Bratton, and P. Tattersall. 1995. The VP1 specific region of MVM is predominantly sequestered within the virus particle. 6th Parvovirus Workshop, Montpellier, France.
- Fisher, A. J., and J. E. Johnson. 1993. Ordered duplex RNA controls capsid architecture in an icosahedral animal virus. *Nature*. 361:176–179.
- Goldberg, M. 1937. A class of multi-symmetric polyhedra. *Tohoku Math. J.* 43:104–108.
- Golmohammadi, R., K. Valegard, K. Fridborg, and L. Liljas. 1993. The refined structure of bacteriophage MS2 at 2.8 Å resolution. *J. Mol. Biol.* 234:620–639.
- Griffith, J., D. Griffith, I. Rayment, W. T. Murakami, and D. L. D. Caspar. 1992. Inside polyomavirus at 25 Å resolution. *Nature*. 355:652–654.
- Harrison, S. C., J. J. Skehel, and D. C. Wiley. 1996. Virus structure. In *Virology*, 3rd Ed. B. N. Fields, D. M. Knipe, P. M. Howley, editors. Raven Press, New York. 59–99.
- Hendrickson, W. W. 1985. Stereochemically restrained refinement of macromolecular structures. *Methods Enzymol.* 115:252–270.

- Jones, T. A., J.-Y. Zou, S. W. Cowan, and M. Kjeldgaard. 1991. Improved methods for building protein models in electron density maps and the location of errors in these models. *Acta Crystallogr.* A47:110–119.
- Kajigaya, S., H. Fujii, A. Field, S. Anderson, S. Rosenfeld, L. J. Anderson, T. Shimada, and N. S. Young. 1991. Self-assembled B19 parvovirus capsids, produced in a baculovirus expression system, are antigenically and immunogenically similar to native virions. *Proc. Natl. Acad. Sci. USA.* 88:4646–4650.
- Kurtzman, G. J., N. Frickhofen, J. Kimball, D. W. Jenkins, A. Nienhuis, and M. S. Young. 1989. Pure red-cell aplasia of 10 years' duration due to persistent parvovirus B19 infection and its cure with immunoglobulin therapy. *N. Engl. J. Med.* 321:519–523.
- Larson, S. B., S. Koszelak, J. Day, A. Greenwood, J. A. Dodds, and A. McPherson. 1993. Double-helical RNA in satellite tobacco mosaic virus. *Nature.* 361:179–182.
- Liddington, R. C., Y. Yan, J. Moulai, R. Sahli, T. L. Benjamin, and S. C. Harrison. 1991. Structure of simian virus 40 at 3.8-Å resolution. *Nature.* 354:278–284.
- Luzzati, V. 1952. Traitement statistique des erreurs dans la détermination des structures cristallines. *Acta Crystallogr.* 5:802–810.
- Marks, R. W. 1960. *The Dymaxion World of Buckminster Fuller.* Reinhold, New York.
- McKenna, R., L. L. Ilag, and M. G. Rossmann. 1994. Analysis of the single-stranded DNA bacteriophage ϕ X174, refined at a resolution of 3.0 Å. *J. Mol. Biol.* 237:517–543.
- Pattison, J. R. 1990. Parvoviruses: medical and biological aspects. *In* Virology. B. N. Fields, D. M. Knipe, editors. Raven Press, New York. 1765–1784.
- Rayment, I., T. S. Baker, D. L. D. Caspar, and W. T. Murakami. 1982. Polyoma virus capsid structure at 22.5 Å resolution. *Nature.* 295:110–115.
- Rimmelzwaan, G. F., M. C. M. Poelen, R. H. Meloen, J. Carlson, F. G. C. M. UytdeHaag, and A. D. M. E. Osterhaus. 1990. Delineation of canine parvovirus T cell epitopes with peripheral blood mononuclear cells and T cell clones from immunized dogs. *J. Gen. Virol.* 71:2321–2329.
- Rosenfeld, S. J., K. Yoshimoto, S. Kajigaya, S. Anderson, N. S. Young, A. Field, P. Warrener, G. Bansal, and M. S. Collett. 1992. Unique region of the minor capsid protein of human parvovirus B19 is exposed on the virion surface. *J. Clin. Invest.* 89:2023–2029.
- Rossmann, M. G. 1995. *Ab initio* phase determination and phase extension using non-crystallographic symmetry. *Curr. Opin. Struct. Biol.* 5:650–655.
- Rossmann, M. G., and J. E. Johnson. 1989. Icosahedral RNA virus structure. *Annu. Rev. Biochem.* 58:533–573.
- Studdert, M. J. 1990. Tissue tropism of parvoviruses. *In* Handbook of Parvoviruses, Vol. 2. P. Tijssen, editor. CRC Press, Boca Raton, FL. 27–32.
- Tattersall, P., A. J. Shatkin, and D. C. Ward. 1977. Sequence homology between the structural polypeptides of minute virus of mice. *J. Mol. Biol.* 111:375–394.
- Tsao, J., M. S. Chapman, M. Agbandje, W. Keller, K. Smith, H. Wu, M. Luo, T. J. Smith, M. G. Rossmann, R. W. Compans, and C. Parrish. 1991. The three-dimensional structure of canine parvovirus and its functional implications. *Science.* 251:1456–1464.
- Valegard, K., J. Murray, P. Stockley, N. Stonehouse, and L. Liljas. 1994. Crystal structure of an RNA bacteriophage coat protein-operator complex. *Nature.* 371:623–626.
- Witherell, G. W., J. M. Gott, and O. C. Uhlenbeck. 1991. Specific interaction between RNA phage coat proteins and RNA. *Prog. Nucleic Acid Res. Mol. Biol.* 40:185–220.
- Wu, H., W. Keller, and M. G. Rossmann. 1993. Determination and refinement of the canine parvovirus empty-capsid structure. *Acta Crystallogr.* D49:572–579.
- Wu, H., and M. G. Rossmann. 1993. The canine parvovirus empty capsid structure. *J. Mol. Biol.* 233:231–244.
- Xie, Q., and M. S. Chapman. 1996. Canine parvovirus capsid structure, analyzed at 2.9 Å resolution. *J. Mol. Biol.* 264:497–520.
- Zhou, G., J. Wang, E. Blanc, and M. S. Chapman. 1997. Determination of the relative precision of atoms in a macromolecular structure. *Acta Crystallogr.* (in press).